Aspects of computer-aided detection (CAD) and volumetry of pulmonary nodules using multislice CT

ARTICLE *in* BRITISH JOURNAL OF RADIOLOGY · FEBRUARY 2005

Impact Factor: 2.03 · DOI: 10.1259/bjr/30281702 · Source: PubMed

8 AUTHORS, INCLUDING:

Rafael Wiemker
Philips
102 PUBLICATIONS **905** CITATIONS
SEE PROFILE

Patrik Rogalla
University Health Network
283 PUBLICATIONS **3,140** CITATIONS
SEE PROFILE

Ori Hay
Tel Aviv University
13 PUBLICATIONS **149** CITATIONS
SEE PROFILE

Thorsten R Fleiter
University of Maryland Medical Center
96 PUBLICATIONS **1,092** CITATIONS
SEE PROFILE

The British Journal of Radiology, 78 (2005), S46–S56
DOI: 10.1259/bjr/30281702

Aspects of computer-aided detection (CAD) and volumetry of pulmonary nodules using multislice CT

[1]R WIEMKER, PhD, [2]P ROGALLA, MD, [1]T BLAFFERT, PhD, [3]D SIFRI, MSc, [3]O HAY, MSc, [4]E SHAH, MSc, [5]R TRUYEN, MSc and [6]T FLEITER, MD

[1]*Philips Research Laboratories Hamburg, Germany,* [2]*Department of Radiology, Charité Hospital, Humboldt University Berlin, Germany,* [3]*Philips Medical Systems CT, Haifa, Israel,* [4]*Philips Medical Systems CT Clinical Science, Cleveland, OH, USA,* [5]*Philips Medical Systems Medical IT, Best, The Netherlands and* [6]*University Hospitals of Cleveland, Ohio, USA*

Abstract. With the superb spatial resolution of modern multislice CT scanners and their ability to complete a thoracic scan within one breath-hold, software algorithms for computer-aided detection (CAD) of pulmonary nodules are now reaching high sensitivity levels at moderate false positive rates. A number of pilot studies have shown that CAD modules can successfully find overlooked pulmonary nodules and serve as a powerful tool for diagnostic quality assurance. Equally important are tools for fast and accurate three-dimensional volume measurement of detected nodules. These allow monitoring of nodule growth between follow-up examinations for differential diagnosis and response to oncological therapy. Owing to decreasing partial volume effect, nodule volumetry is more accurate with high resolution CT data. Several studies have shown the feasibility and robustness of automated matching of corresponding nodule pairs between follow-up examinations. Fast and automated growth rate monitoring with only few reader interactions also adds to diagnostic quality assurance.

Pulmonary nodules are among the most common focal pulmonary lesions [1]. The presence or absence of pulmonary nodules can be of great value in the differential diagnosis of lung diseases [2]. Therefore, the detection and diagnosis of pulmonary nodules in CT data sets of the thorax is a standard procedure in radiological practice. Pulmonary nodules are often benign, or may be metastases from various cancer types, but they may also be an indication for primary lung cancer. Cancer of the lung and bronchus (hereafter, lung cancer) is the second most common type of cancer. However, owing to its aggressiveness, lung cancer is the number one cause of all cancer-related deaths, with more than 150 000 deaths in the USA each year [3].

Early detection of lung nodules is crucial both for close observation or biopsy to differentiate between benign or malignant nodules and for timely therapy. Among the most common methods to detect pulmonary nodules are chest radiography and CT. Fibre optic bronchoscopy is also used but has limited value for finding nodules other than those in the larger airways. CT offers better contrast than chest radiography between nodule and background, with no overlapping structures, and several studies have shown that CT can detect smaller, earlier stage nodules with a higher sensitivity than chest radiography [4].

Recently, CT technology has undergone a major evolution with the introduction of multislice technology. With multislice CT (MSCT), a full lung, thin slice ($<$1 mm) scan can be performed within a single breath-hold. It is hoped that with the high resolution CT data available from MSCT scanners, cancerous nodules can be recognised while still small and in an early stage of lung cancer. Many researchers assume that this downstaging effect by early detection of lung cancer will ultimately improve the survival rate [5, 6].

Moreover, it is hoped that lung cancer screening of high-risk patient groups may significantly increase the rate of lung cancer cases that are diagnosed before the cancer has metastasised. These propositions will be investigated during a large-scale randomised 9-year trial conducted by the US National Cancer Institute (NCI): the currently starting National Lung Screening Trial (NLST) will enrol 50 000 current or former smokers and will take place at a total of 30 sites throughout the USA [http://www.cancer.gov/newscenter/NLSTQA].

Two main areas must be distinguished where computer assistance can be used. First, there is the computer-aided detection (CAD) of pulmonary nodules as such, be they malignant or benign, calcified, solid or subsolid. The results of CAD are markers that draw the attention of the reader to locations of suspicious anomalies. In the context of CAD, a marker is considered as a true positive even if it points at a benign or calcified nodule; false positive markings are then those that do not point at nodules at all (but at scars, bronchial wall thickenings, motion artefacts, vessel bifurcations, etc.). The outcome of CAD is not a yes/no decision, but rather markings at certain locations; therefore the term ''true negative'' is not defined and a normalised specificity cannot be given. Instead, the performance of CAD is usually given as a sensitivity (detection rate) and a false positive rate (false positive markings per CT study).

The second area is computer-aided diagnosis (often abbreviated as CADx) and aims at the differential diagnosis between malignant and benign pulmonary nodules. Only a fraction of the pulmonary nodules are malignant carcinomas from lung cancer or metastases

from cancers in other organs. It is well known that the fraction of nodules that are actually malignant decreases when smaller and smaller nodules are considered [5, 6] as they become detectable by the still increasing resolution of MSCT scanners.

A number of different clinical approaches are aimed at differential diagnosis: biopsy, observation of possible growth by follow-up examinations [7], appraisal of morphological features (such as spiculated or smooth margins), measurement of contrast enhancement in a dynamic CT series [8, 9], and use of additional modalities such as positron emission tomography (PET), etc. For all these clinical approaches, software modules for computer-aided quantification can be used, not only to speed up the workflow, but also to make the necessary measurements themselves more accurate, less prone to error and more repeatable. Going beyond pure quantification, CADx software can then compare the measured values in a multidimensional feature space to known benign and malignant example populations, and retrieve similar cases with known diagnosis from a database or give a likelihood estimation for malignancy [10]. In the context of CADx, false positives are then nodules that are judged to be malignant while really being benign nodules. CADx faces a classical yes/no decision problem, or at least an outcome range that can be normalised to a 0 to 1 interval, so that its performance can be rated by normalised sensitivity and specificity.

Among the various needs for quantification of lung nodules, volume measurement (volumetry) of a detected nodule is the most immediate (for reporting) and the most basic (for detection of possible growth in a follow-up examination).

As a software technology, CAD and volumetry aims at three main objectives.

- Diagnostic quality assurance: by detecting and marking suspicious lesions, CAD can help to avoid potential nodules from being overlooked by the radiologist.
- To increase therapy success by early detection of cancer: by downstaging the typical stage when a cancer is diagnosed; it is hoped that detection at an earlier stage increases the survival rates.
- Reduction of biopsies: by computation of growth rates and doubling times of lung nodules between follow-up examinations, many of the detected nodules can be evaluated non-invasively to avoid the risks associated with invasive procedures such as needle biopsies.

From a technical point of view, a number of separate technical tasks can assist the reading radiologist, the underlying principles, problems and results of which we will address in this paper:

- automated detection of lung nodules;
- automated three-dimensional volumetry;
- automated image registration (alignment) of the lungs between previous and follow-up scan, and matching of the locations of each nodule in both data sets.

This paper resulted from a presentation at the British Institute of Radiology on current developments in CAD of pulmonary nodules. The aim of this paper is to show that computer-aided detection and quantification of pulmonary nodules have reached a maturity level such as to significantly contribute to quality of clinical diagnosis.

Computer-aided detection (CAD)

Lung nodules can be detected particularly well by CT, since they show good contrast in the lung parenchyma and, in contrast to projection radiography, cannot be hidden by ribs etc. However, although in principle detectable with CT, a non-negligible fraction of small nodules may be overlooked by the radiologist, particularly if they are located centrally and hidden in a maze of vessels of similar size (Figure 1). This may be even the more so, as modern multislice scanners can produce up to 1000 slices for a thoracic CT examination, where all the small vessels showing up in the isotropic submillimetre resolution have to be checked for their three-dimensional (3D) connectivity to rule out the presence of possible nodules. Therefore, computer assistance for detecting lung nodules in CT data sets is a straightforward concept and has been suggested and investigated as early as 1989 [11–13]. The underlying idea is not that the diagnosis is delegated to a machine, but rather that a machine algorithm acts as a support to the radiologist and points out locations of suspicious objects, so that the overall sensitivity (detection rate) is raised. This could be particularly important in screening situations, with a massive reviewing load of CT studies.

CAD following the advent of MSCT

The large majority of computer-aided lung nodule detection approaches in the last decade have been designed for and tested on conventional 5–10 mm CT slice thickness [14–22]. However, the reported sensitivity and specificity rates were often disappointingly low and failed to reach the level of clinical acceptance and usefulness. On the one

Figure 1. Example of a central lung nodule (4 mm diameter) hidden in the maze of the pulmonary vessel tree (maximum intensity projection).

hand, the detection rate was not sufficient, while on the other hand the false positive rate was sometimes so high that it annoyed and tired radiologists to the point of negating any potential gain in sensitivity. For example, a typical study on 10-mm slice thickness CT data [17] reports only 38% sensitivity (on 68 nodules) with six false positives per patient. Another study [16] reports 72% sensitivity (on 98 nodules) with 31 false positives per patient. Moreover, both studies have restricted themselves to nodules with diameters $\geqslant 5$ mm.

The principal problem of computerised nodule detection in thick slices of 5–10 mm is that the opacity of nodules that are smaller than the slice thickness is reduced to subsolid appearance by the partial volume effect. Therefore it is impossible to set a certain Hounsfield value as a threshold for potential nodules. Rather, many different thresholds have to be tried [18], and false positives cannot be rejected simply owing to a low Hounsfield value. Another problem with thick CT slices is that a reasoning mechanism is required to recognise constellations where a small nodule is overshadowed by a vessel of similar size within the 10 mm projection [22]. Also, thin vessels may appear disconnected when running obliquely through the slice images and thus be mistaken for nodules.

With the advent of MSCT scanners it is now possible to obtain thin slice CT image data (*e.g.* 1 mm slice thickness) for the whole thorax within a single breath-hold (Figure 2). For example, at 60 mm coverage per second for a 40-slice scanner (detector coverage 40×0.625 mm$=25$ mm, at pitch 1, no overlap, 0.42 rotations per second), it takes less than 10 s to cover the entire lung area. Owing to the short recording time, multislice high resolution CT data have relatively low motion artefacts, and with a slice thickness $\leqslant 1$ mm allow the detection of very small nodules.

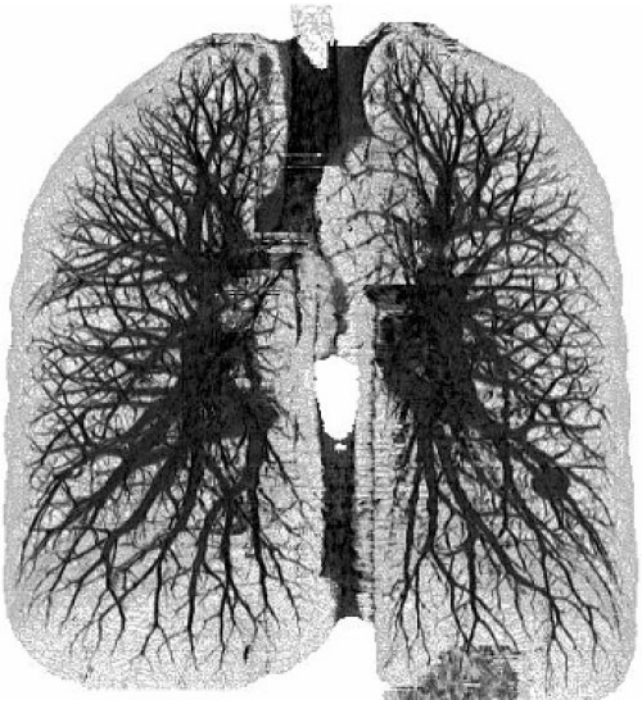

Figure 2. Vessels and airways of the lung, visualised after automated segmentation of a high resolution CT data set (1 mm slice thickness, 400 slices, inverted maximum intensity projection).

At first, high resolution CT (HRCT) was used mainly for segmentation, characterisation and classification of already singled-out individual nodules [23–27]. More recently HRCT data have also been used for nodule detection (in contrast to nodule segmentation) within a complete thorax data set [28–30].

The obvious advantage of HRCT data is that with voxel spacings as fine as $0.5 \times 0.5 \times 0.5$ mm^3 the partial volume effect vanishes for nodules of size >1 mm (at least for the central voxel). Thus, the Hounsfield values can be evaluated as absolute attenuation values, and the fully isotropic 3D shape information of potential nodules can be utilised by CAD algorithms to resolve ambiguities between pulmonary nodules and vessels.

The CAD algorithm we have suggested in reference [30] works on pure geometric reasoning. It assumes that any blob-like solid structure (which may on one side be attached to a plane-like structure, the lung wall) may be a candidate for a pulmonary nodule if all connecting vessels are significantly smaller in diameter than the central blob-like structure.

For efficiency reasons, these criteria are first checked in the 2D slice images. From each of the resulting seed points, a 3D region-growing procedure is then started to distinguish nodules from vessels that continue with approximately constant diameter, as for nodules it is expected that any connecting vasculature will be decreasing rapidly in diameter. To allow for the wide range of anatomical variability of pulmonary nodules, we use a combination of several geometric descriptors to decide whether a candidate will finally be judged to be a highly likely nodule candidate to be marked by the CAD system.

CAD results on clinical data: detection rate and false positive rate

A pilot study of a lung nodule CAD system (Philips Research, Hamburg, Germany) was conducted on images from the Radiology Department at the Charité University Hospital in Berlin [30]. The images were acquired in the years 2000–2001 by a 4-slice scanner over the entire thorax at 120 kV and 100 mAs.

Each thorax data set comprised 300–500 slice images with 512×512 pixels. The x-y-resolution (inslice) varied between 0.5 mm and 1.0 mm, and the z-resolution (reconstruction interval) varied between 0.5 mm and 1.0 mm, with a slice thickness of 1 mm (slightly overlapping slices). In addition to the radiologist, the thoracic data sets were read by the CAD software (computation time was approximately 1 min for all 300–500 slices per thorax). The CAD software marks possible nodules on the axial slice images (Figure 3) and gives an overview of all found nodule candidates for inspection by the radiologist (Figures 4 and 5).

In total, 12 patients and 330 nodule candidates were analysed (for examples see Figures 6–8). All nodule candidates were above -400 Hounsfield units (HU), including pleural nodules (Figure 7). Comparison was carried out per nodule for calculation of true and false positives, false negatives, and with respect to nodule size.

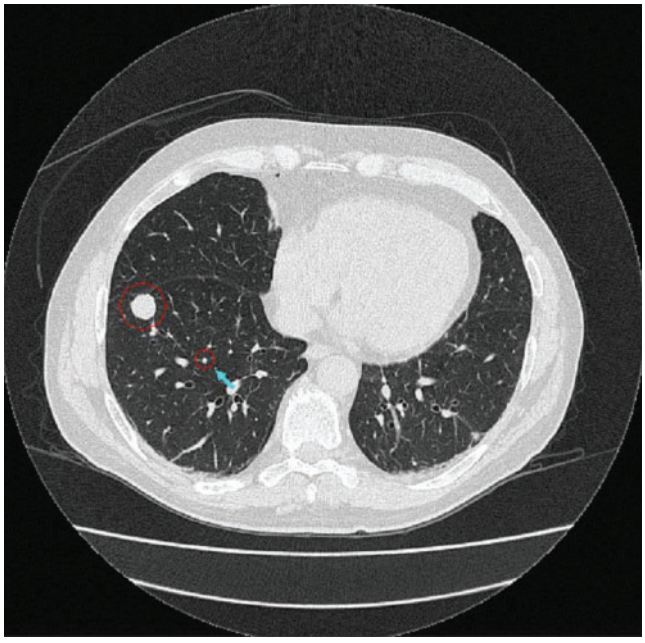

Figure 3. Computer-detected nodule candidates (here a large nodule and a more subtle one, which is also three-dimensionally rendered in Figure 8) are marked on the axial slice images.

The automated detection showed a sensitivity of 84% (detection rate including nodules of all sizes). If the minimum nodule size for detection was set to 2 mm, the sensitivity was 95% with 4.4 false positives per patient. For nodules greater than 4 mm, the sensitivity was 96% with 0.5 false positives per patient.

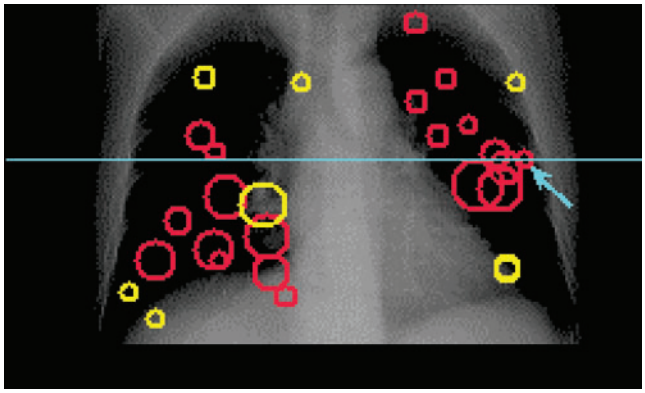

Figure 4. Overview of the computer-detected nodules indicated in a coronal view of the thorax CT data set.

However, we would not necessarily expect such a high detection rate at an equally low false positive rate in all clinical settings. Examinations may be taken with low dose or ultra low dose imaging protocols, patient compliance to not breath or move may be less, and moreover the delineations and regularity of the nodule population in question may vary considerably.

CAD performance comparison

Experience with clinical studies has shown that the measured detection rates achieved by CAD systems as well as by radiologists themselves clearly depend on the number of co-reading radiologists: the more co-readers participating, the more suspicious lesions will inevitably be found,

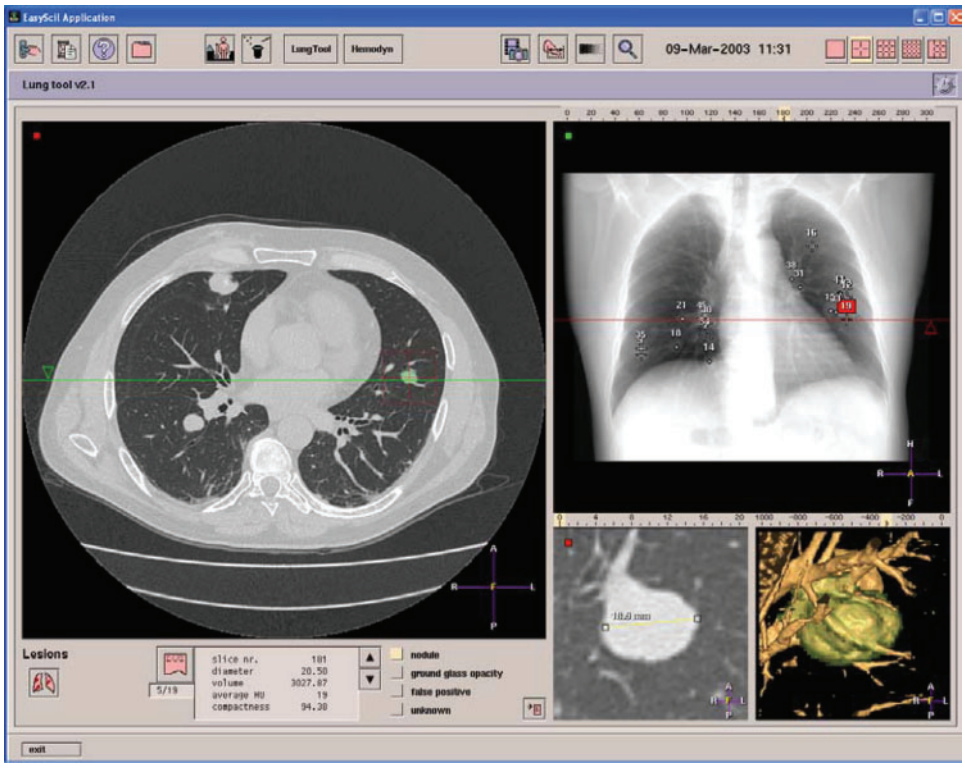

Figure 5. Graphical user interface for inspection of the computer-detected nodules. A mouse click on a nodule yields a close-up window with a rotatable slab maximum intensity projection and the volume rendering of the automatically segmented nodule (bottom right).

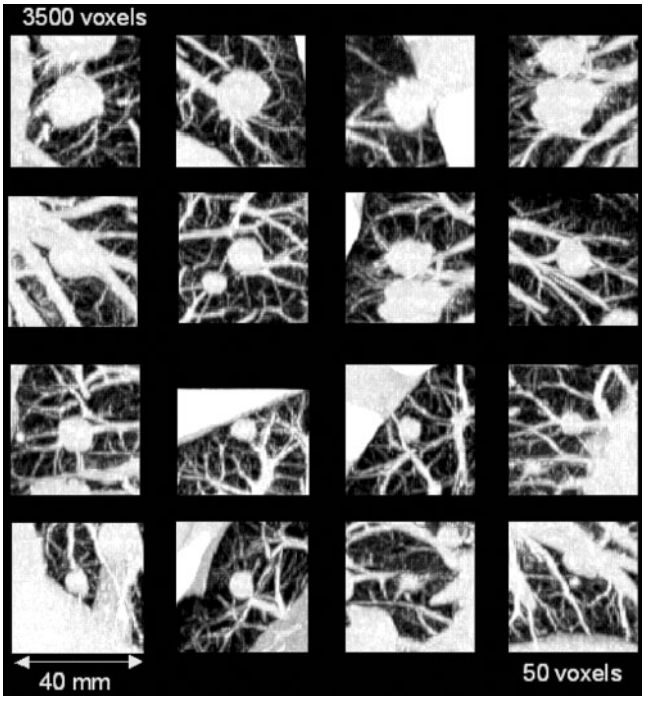

Figure 6. Maximum projection renderings of a variety of pulmonary nodules of different sizes (ordered by volume from top left to bottom right). The wide spectrum of possible sizes is one of the challenges that had to be mastered for computer detection algorithms.

and thus the individual sensitivity of each participating radiologist and CAD system will decrease. But even though the absolute sensitivity figures have to be appreciated with care, all clinical studies have agreed that a significant number of nodules have been detected by the additional CAD software alone, while being overlooked by all co-reading radiologists [30–33]. Therefore, CAD can be seen as a strong quality assurance tool.

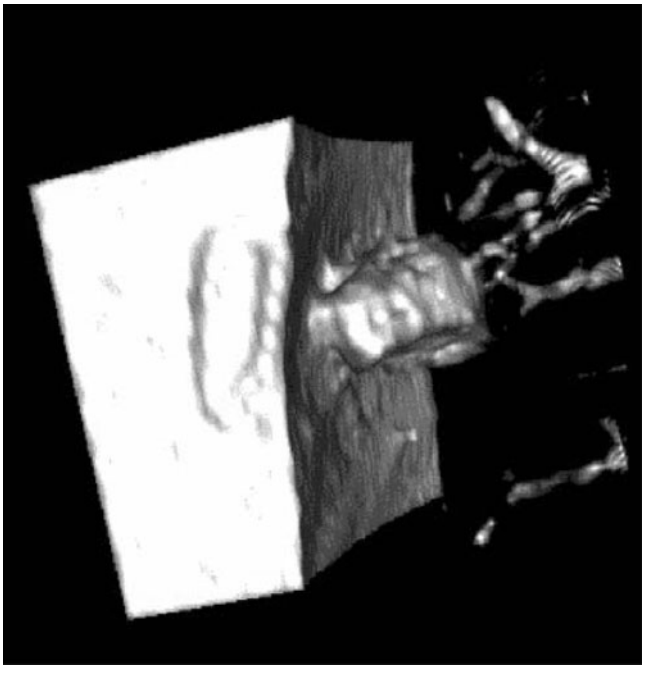

Figure 7. Volume rendering of a juxta-pleural nodule with attached vessels.

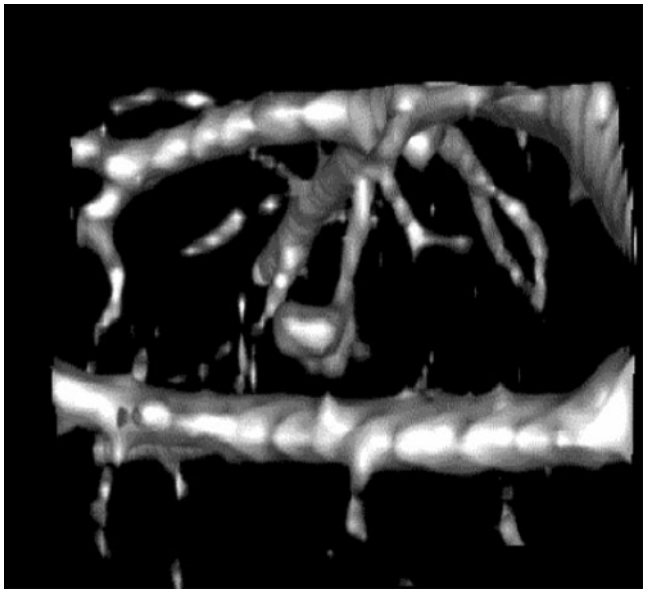

Figure 8. Volume rendering of a central nodule (4 mm) with attached vessels.

Up to now it is hard to compare the performance of the different CAD algorithms, as they have all been tested in different settings, on different patient data sets, and acquired with different scanners and imaging protocols.

To allow a more objective comparison of CAD performance, the NCI has formed a consortium to build up a lung image database with consensus-based diagnostic findings [http://www3.cancer.gov/bip/lidc_comm.htm], which could then be used to validate and improve CAD software [34].

Typical false positive findings

In medical terminology, benign pulmonary nodules that do not require action are sometimes called false positives. However, in the context of CAD, the term false positive means locations that are indicated by the CAD algorithm but are not nodules at all. Typical false positive markings are:

- artefacts from respiratory or cardiac motion, *e.g.* vessels that are running close to the heart and are seemingly disrupted by cardiac motion, and thus appear as a series of small isolated nodules;
- thick vessel bifurcations;
- strongly bent vessels;
- hilus vessels that branch out of the mediastinum and decrease rapidly in diameter so that they are mistaken as pleural nodules with connecting vessels;
- scars in the parenchymal tissue.

Since one of the major sources for false positive nodule markings is cardiac motion artefacts, it is clear that the false positive rate can be significantly reduced by using electrocardiography (ECG)-gated CT studies. In a small

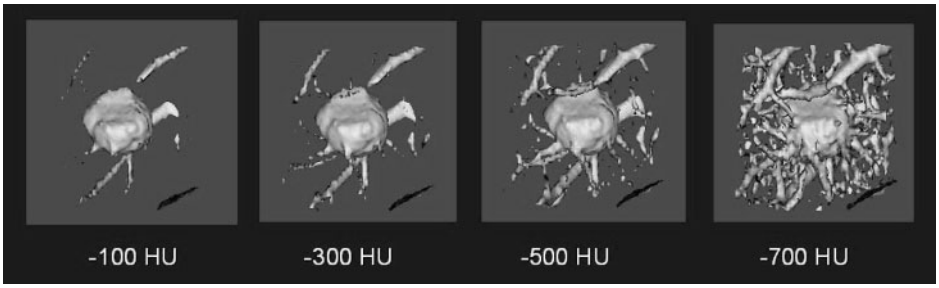

Figure 9. Example of a single nodule as it appears above different Hounsfield thresholds: the vascular connectivity increases with decreasing Hounsfield threshold (surface renderings, CT data: 0.8 mm slice spacing, 1 mm slice thickness).

pilot study at the Cleveland University Hospitals, we have obtained ECG-gated CT scans from a Philips 16-slice scanner. To find the optimal point in the cardiac cycle, the image volumes were reconstructed at 0%, 25%, 50%, 75% and 88% of the R–R cycle. These scans were then subjected to a lung nodule CAD module [30] and the results were compared with a reference reading of two radiologists. The false positive rate varied between 3.5 false positives per patient in the 88% phase and 6 false positives per patient in the 25% phase. This indicates that performance of CAD can be significantly improved by using ECG-gated CT studies reconstructed in the late diastole. However, the additional burden of ECG gating in terms of costs, examination time and exposure dose can probably not be tolerated in all clinical circumstances, *e.g.* in lung cancer screening.

In summary, utilisation of HRCT data from multislice scanners for computer-aided nodule detection holds the promise of increasing sensitivity while minimising false positives in such a way as to achieve a breakthrough for CAD in clinical practice.

Computer-aided volumetry of pulmonary nodules

Nodule volumetry is important for monitoring the success of cancer therapy, as well as to evaluate the growth rate of small indeterminate nodules to evaluate the likelihood of malignancy. Particularly the latter becomes even more important with the increasing number of small nodules detected by visual inspection and CAD in thin slice CT data [35].

The aim is to detect malignancy at as early a stage as possible on the one hand, but to avoid unnecessary biopsies on the other hand.

The advent of thin slice data from multi-array CT scanners has enabled fully automated 3D segmentation and volume measurement of lung nodules.

3D volumetry promises a better sensitivity to growth than manually-guided diameter measurements in a single image slice, since an actual doubling of the nodule volume means a diameter increase of a factor of only $\sqrt[3]{2}$ or 26%, which for small nodules might easily be overlooked in the measurement error range.

Slice-wise manual delineation of the nodules through several adjacent slices is a tedious task and is operator-dependent. To improve workflow and reproducibility, algorithms for fully automated 3D computer-aided segmentation and volume measurement of nodules in CT data sets have been proposed [24, 36–39].

Measuring the 3D nodule volume falls into two different sub-problems.

- The general accuracy of volume measurement depends on the spatial CT resolution (inplane resolution, slice thickness, slice spacing, pitch), as well as on partial volume effect, dose, choice of reconstruction filters, Hounsfield threshold, etc.
- Lung nodules often cannot be delineated unambiguously, as they may be connected to vessels, the lung wall, the diaphragm or the mediastinum (Figures 7 and 8). Therefore, an automated algorithm has to make consistent decisions regarding where to cut off the tumour from the surrounding vasculature. These cut-off decisions will always be somewhat arbitrary, but have to be as consistent as possible in order to allow comparisons between different nodules, and even more important between the same nodule as imaged in the baseline and a later follow-up CT scan. This is not a trivial requirement, as not only the volume but also the morphology of a nodule may have changed during a given time interval (*e.g.* by angiogenesis).

Computer-aided volumetry gives rise to a number of questions that we want to address in this section.

- How accurate is the volume measurements of artificial objects (phantoms) with known real volume?
- Does the accuracy depend on the dose used for the scan?
- Does computer-aided volumetry give the same results as careful manual 3D segmentation?
- How does computer-aided volumetry depend on the slice thickness used for the CT scan? Can measurements be compared between scans with different imaging parameters?

The choice of the Hounsfield threshold above which to account for the nodule volume is a crucial parameter, as the number of visible attached vessels increases with decreasing Hounsfield threshold (see Figure 9). The slice thickness also plays a role: with decreasing slice thickness of the CT image data, more and more surrounding vasculature connecting to the nodules becomes visible that has to be cut off by the segmentation algorithm (see Figure 10). In thick slice data, the connecting vessels can be cut off by raising the Hounsfield threshold [36]. This implicitly utilises the partial volume effect, which assigns lower Hounsfield unit values to thin vessels. This principle does not work in the isotropic resolution of thin slice CT,

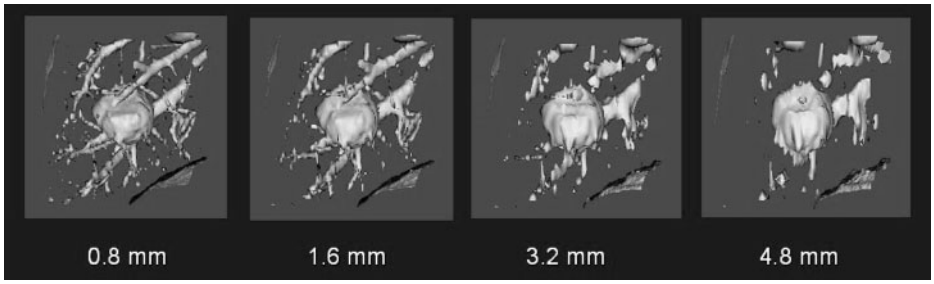

Figure 10. Example of a single nodule as it appears in different slice thicknesses (simulated from original data of 1 mm slice thickness): the vascular connectivity decreases with increasing slice thickness (surface renderings at a threshold of −500 HU).

and several algorithms to cope with this problem have been proposed [24, 36–39]. A method to determine the Hounsfield threshold that yields the strongest gradient between nodule and surrounding parenchyma was proposed by Wiemker and Zwartkruis [40].

In our previous publication [39] we have suggested a volumetry algorithm that starts out from a given seed point selected either manually by mouse click or by the CAD module. The seed point does not necessarily need to be in the centre of the nodule. The software module then starts a 3D region growing process (see Figure 11). The region growing first grows into all areas that are spherical or lobular around the current seed point. Then, from all boundary points of the current region expansion, a further seed point is automatically chosen that is closest to the centre of the surrounding mass, and from here the region growing continues into all areas that are spherical or lobular around the current seed point. This iterative scheme ensures that the region growth first expands into all ''roundish'' parts of the nodule, and only later also grows into the attached tubular vessel structures and possibly into adjacent flat parts of the lung wall (see Figure 11). The growth process stops only after it has grown far from the original start seed point. Then, a retrospective decision is taken regarding where the optimal cut-off point during the growth process would have been. We propose to choose the cut-off point such that the structures that are attached to the nodule are cut through at their thinnest connection, or in the case of an attached lung wall, at the strongest inflection. As an objective function we therefore propose the surface integral over the distance values of the 2D surface of the current 3D region

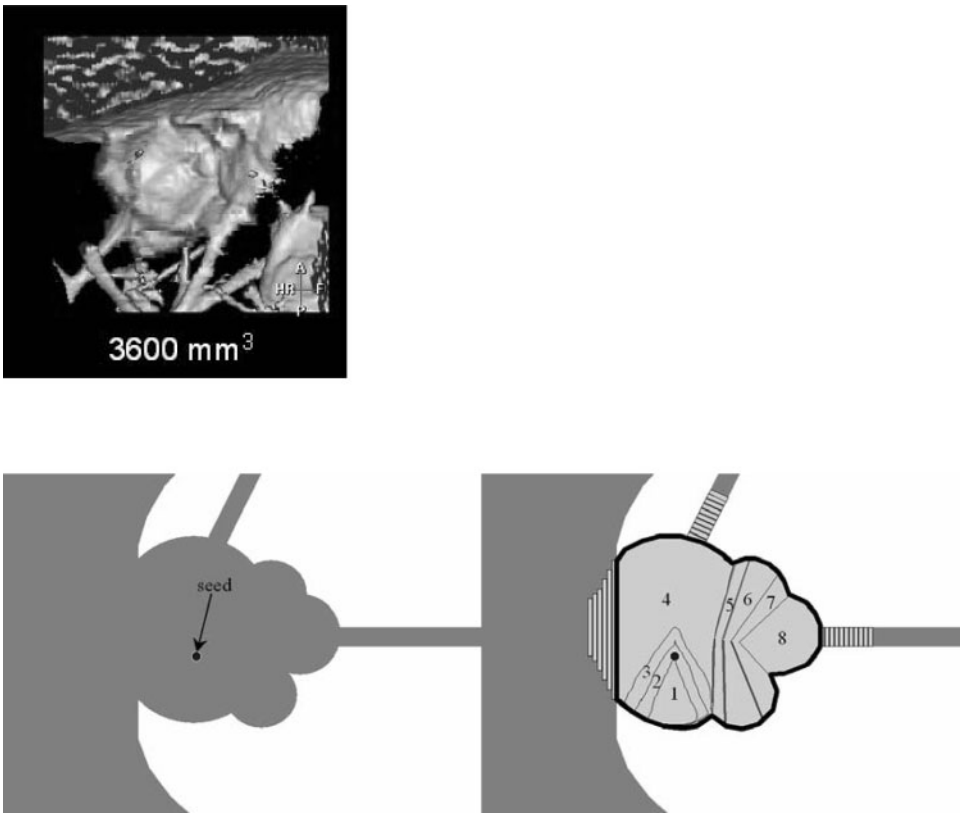

Figure 11. Top: Example of a true nodule attached to the lung wall. Bottom: Sketch of such a nodule to illustrate the segmentation algorithm; left: start point is set, not necessarily at the centre of the mass; right: the areas that are iteratively added to the region expansion, growing first into lobular areas, but then eventually also into the lung wall and connected vessels. The final cut-off surface is denoted by a solid black line.

expansion, where the distance value for each point is defined as the distance between this point and the closest outside nodule point (the surrounding "dark" parenchyma tissue).

This cut-off objective function works in the same way for isolated nodules, or for nodules attached to vessels, the lung wall or diaphragm, and does not require prior segmentation of the lung.

For the proposed nodule segmentation algorithm, we have studied the effect of slice thickness on the measured nodule volume in order to determine the consistency and comparability of nodule volumes measured during follow-up examinations [39]. Considering the delicate vasculature network around the pulmonary nodules, the robustness of computer-aided nodule segmentation algorithms cannot be validated on data from CT phantoms with smooth boundaries only.

Analysis of 41 nodules between 150 mm^3 and 350 mm^3 (6.6–8.7 mm effective diameter) showed that the connectivity of the nodules to the surrounding vasculature clearly increases with thinner slice thickness, so the segmentation algorithm has to cut off more and more thin vessels. On the other hand, in the finest slice spacing there is the weakest dependency of the nodule volume on the Hounsfield threshold (owing to the diminishing partial volume effect). The cut-off decisions for surrounding vessels to be made by the algorithm are different for each Hounsfield threshold, as more or less vessels are visible above a given threshold. Nevertheless, we found that the segmentation algorithm yielded consistent volume estimations with varying slice thicknesses using a threshold of −400 HU. The average variation in volume estimation stayed within 3%. This confirms that the proposed segmentation algorithm yields consistent decisions regarding where to cut off the attached vessels. The segmentation algorithm is shown to be robust enough to compare nodule volumes between follow-up CT studies even of different slice thickness.

In another study at the Hematology–Oncology Clinic of Little Rock, Arkansas, we have compared manual segmentation by two radiologists to a computer-assisted automatic segmentation (Lung Nodule Assessment and Comparison Package; Philips Medical Systems, Best, The Netherlands) for 33 nodules, varying in size from 3.3 mm to 30.0 mm effective diameter. The nodules were classified as difficult or isolated based on whether they were attached to vessels, lung wall, or close to other nodules or scar tissue. Several types of nodules such as solid, spiculated and calcified were included in the study. Using identical image window, level and image zoom, both radiologists drew contours along the boundaries of nodules in every axial image in which the nodule is present. All nodule images were acquired at 16×0.75 mm collimation and reviewed at 1 mm slice width and 1 mm increment. The total volume from manual segmentation was calculated by summation of the individual slice-wise contour areas. For automatic segmentation, a seed point was placed on the nodule in only one axial slice.

Comparisons were made of manual measurements between the two radiologists, manual *vs* automated volume segmentation, and time for segmentation using automated and manual methods. The correlation between the manual measurements by two radiologists was 0.987. There was also a strong correlation between automated and manual segmentation, with the correlation coefficient equal to 0.972 and 0.986 for the two radiologists, respectively. Thus the agreement between manual and computer-aided volumetry proved to be equally good as the agreement between the two human readers. The automated measurements required minimal user interaction, with average volume estimation time per nodule of a few seconds. Manual measurements on the other hand took an average of 5 min per nodule.

Another question is how robust computer-aided nodule volumetry is against varying radiation dose. Hay et al [41] have studied the effect of using low dose imaging protocols for lung nodule volumetry. In their phantom study with 34 different artificial spheres and cylinders of different sizes, they found the segmentation accuracy to be better than 5% both for standard dose and low dose CT scans.

In summary, we conclude that for solid nodules, computer-assisted volumetry is accurate, robust, repeatable and consistent. For subsolid nodules (ground-glass opacities) however, definitions of meaningful characterisation still have to be agreed on.

Follow-up registration and matching of nodules

Evaluating the potential growth or shrinkage of pulmonary nodules between a former CT examination and a current follow-up examination is a routine task in radiological practice, not only for diagnosis of detected nodules, but also for monitoring the response to oncological therapy. The typical manual matching procedure is quite time consuming; the user has to separately scroll through the slice stacks of the two studies and locate each nodule and then locate the same nodule in the follow-up study, perform the volumetry and copy down the results. In contrast, the computer-assisted matching indicates the corresponding nodule location in the other data set when the user points to the nodule in either one of the data sets (see Figure 12). Moreover, a list of matching pairs is automatically compiled for all nodules found in the two data sets (detected both manually and/or by CAD).

To perform such a statistical growth analysis with measurement and matching in a manual fashion is of course possible, but might simply not be undertaken for all cases in the clinical practice with high case load pressure, owing to its forbidding time consumption. Therefore, the computer-aided follow-up matching may be more than a convenience tool but indeed may contribute to diagnostic quality assurance.

The automatic nodule matching approach described by Blaffert and Wiemker [42] starts out by segmenting the lungs out of the overall thoracic CT data volume of the current and former study. The two lung volume images are registered (aligned) using an affine coordinate transformation. The similarity between the former and current lung volume is tested by virtue of the cross-correlation of both data sets. The coordinate transformation is then varied until optimal cross-correlation is reached. By using Gauss–Newton optimisation methods in variation of the coordinate transform, and by employing a coarse to fine resolution multiscale approach, the optimal alignment of the two lung volumes can be reached in typically 5 s.

In general, an affine coordinate transformation is not expected to always suffice for the alignment of the same

Figure 12. Example of automated matching of a nodule between follow-up examinations reconstructed with different imaging protocol parameters.

lung between a former and current CT study, since the possibly different respiratory state and patient pose on the CT table may cause elastic deformations. However, elastic image registration is too time consuming at the current state of the art, and the experimental results indicate that affine image registration comes close enough to allow correct matching of the nodule positions in the former and the current study: after alignment of the lungs in the CT study pair, the mean distance between the location of a nodule in the former and the current study was 4 mm [42]. 124 of 125 nodules were correctly matched even if the CT study pairs were recorded with different field of view, slice thickness or slice spacing [43].

Betke et al [44] use a different algorithm and test set and report a mean distance of 8 mm between the location of a nodule after automated image registration, and 56 of 58 nodule pairs correctly matched. Another equally favourable result was given for an algorithm of Shen et al [45].

Conclusion

With the advent of MSCT scanners and their possibility to acquire submillimetre slice data over the whole thorax within a single breath-hold, software algorithms for CAD of pulmonary nodules start to reach a level of sensitivity and specificity that can significantly improve the diagnostic quality and can provide radiology departments with the increased safety of a ''second reader'' at low cost.

As more and smaller lung nodules become detectable in thin slice CT, automated and reproducible computer-aided 3D volumetry of lung nodules becomes important to speed up workflow, to compute growth rates between follow-up examinations and thus to avoid unnecessary biopsies.

With ever refining spatial, dynamic and temporal resolution of CT scanners, more applications of computer-aided detection and quantification are likely to emerge.

Acknowledgments

We would like to thank Noah Weg, MD, of Weg & Associates, Suffern, New York, and Thomas W Koonce, MD, and John E Slayden, MD, of the Hematology–Oncology Clinic of Little Rock, Arkansas, for evaluating the Philips Lung Nodule Assessment and Comparison package.

References

1. Prokop M, Galanski M. Spiral and multislice computed tomography of the body. Stuttgart, Germany: Thieme Medical Publishers, 2003.
2. Webb WR, Müller NL, Naidich DP. High resolution CT of the lung (2nd edn). Philadelphia, PA: Lippincott-Raven Publishers, 1996.
3. Ries LAG, Eisner MP, Kosary CL, Hankey BF, Miller BA, Clegg L, et al. In: Feuer EJ, Edwards BK, editors. SEER Cancer statistics review, 1975–2000. Bethesda, MD: National Cancer Institute. http://www.cancer.gov/statistics [accessed 14 November 2004].
4. Bach PB, Kelley MJ, Tate RC, McCrory DC. Screening for lung cancer: a review of the current literature. Chest 2003;123:72S–82S.
5. Henschke CI, McCauley DI, Yankelevitz DF, Naidich DP, McGuinness G, Miettinen OS, et al. Early lung cancer action project: overall design and findings from baseline screening. Lancet 1999;354:99–105.
6. Diederich S, Wormanns D, Semik M, Thomas M, Lenzen H, Roos N, et al. Screening for early lung cancer with low-dose spiral CT: prevalence in 817 asymptomatic smokers. Radiology 2002;222:773–81.
7. Wormanns D, Diederich S. Characterization of small pulmonary nodules by CT. Eur Radiol 2004;14:1380–91.
8. Swensen SJ, Viggiano RW, Midthun DE, Muller NL, Sherrick A, Yamashita K, et al. Lung nodule enhancement at CT: a multicenter study. Radiology 2000;214:73–80.
9. Wormanns D, Klotz E, Dregger U, Beyer F, Heindel W. Diagnostic performance of different measurement methods for lung nodule enhancement at dynamic computed tomography. Proc. SPIE Medical Imaging Conference 2004. SPIE 2004;5372:455–62.
10. Li F, Li Q, Aoyama M, Shiraishi J, Abe H, Suzuki K, et al. Usefulness of computerized scheme for differentiating benign from malignant lung nodules on high-resolution CT. In: Proceedings of Computer Assisted Radiology and Surgery CARS 2004. Amsterdam, The Netherlands: Elsevier, 2004:946–51.

11. Preteux F, Merlet N, Grenier P, Mouellhi M. Algorithms for automated evaluation of pulmonary lesions by high resolution CT via image analysis. In: Proceedings of Radiological Society of North America RSNA'89. Oak Brook, IL: Radiological Society of North America, 1989:416.
12. Preteux F. A non-stationary Markovian modeling for the lung nodule detection in CT. In: Proceedings of Computer Assisted Radiology CAR 1991. Berlin, Heidelberg, New York: Springer Publishers, 1991:199–204.
13. Giger M, Bae K, MacMahon H. Computerized detection of pulmonary nodules in computed tomography images. Invest Radiol 1994;29:459–65.
14. Lee Y, Hara T, Fujita H, Itoh S, Ishigaki T. Nodule detection on chest helical CT scans by using a genetic algorithm. Proc Intel Inf Systems 1997;67–70.
15. Lee Y, Hara T, Fujita H, Itoh S, Ishigaki T. Automated detection of pulmonary nodules in helical CT images based on an improved template-matching technique. IEEE Trans Medical Imaging 2001;20:595–604.
16. Fiebich M, Wietholt C, Renger B, Armato S, Hoffmann K, Wormanns D, et al. Automatic detection of pulmonary nodules in low-dose screening thoracic CT examinations. In: Proceedings of SPIE Medical Imaging Conference 1999. SPIE 1999;3661:1434–9.
17. Fiebich M, Wormanns D, Heindel W. Improvement of method for computer-assisted detection of pulmonary nodules in CT of the chest. In: Proceedings of SPIE Medical Imaging Conference 2001. SPIE 2001;4322:702–9.
18. Armato S, Giger M, Moran C, Blackburn J, Doi K, MacMahon H. Computerized detection of pulmonary nodules on CT scans. Radiographics 1999;19:1303–11.
19. Armato S, Giger M, Blackburn J, Doi K, MacMahon H. Three-dimensional approach to lung nodule detection in helical CT. In: Proceedings of SPIE Medical Imaging Conference 1999. SPIE 1999;3661:553–9.
20. Armato S, Giger M, MacMahon H. Analysis of a three-dimensional lung nodule detection method for thoracic CT scans. In: Proceedings of SPIE Medical Imaging Conference 2000. SPIE 2000;3979:103–9.
21. Satoh Y, Ukai N, Niki K, Eguchi K, Mori H, Ohmatsu R, et al. Computer aided diagnosis system for lung cancer based on retrospective helical CT image. In: Proceedings of SPIE Medical Imaging Conference 1999. SPIE 1999;3661: 1324–35.
22. Takizawa H, Fukano G, Yamamoto S, Matsumoto T, Tateno Y, Iinuma T, et al. Recognition of lung cancers from X-ray CT images considering 3-D structure of objects and uncertainty of recognition. In: Proceeding of SPIE Medical Imaging Conference 2000. SPIE 2000;3979:998–1007.
23. Reeves A, Kostis W, Yankelewitz D, Henschke C. Three-dimensional shape characterization of solitary pulmonary nodules from helical CT scans. In: Proceedings of Computer Assisted Radiology and Surgery CARS 1999. Amsterdam, The Netherlands: Elsevier, 1999:83–7.
24. Kostis W, Reeves A, Yankelewitz D, Henschke C. Three-dimensional segmentation of solitary pulmonary nodules from helical CT scans. In: Proceedings of Computer Assisted Radiology and Surgery CARS 1999. Amsterdam, The Netherlands: Elsevier, 1999:203–7.
25. Kawata Y, Niki N, Ohmatsu H, Kusumoto M, Kakinuma R, Mori K, et al. Curvature based characterization of shape and internal intensity structure for classification of pulmonary nodules using thin-section CT images. In: Proceedings of SPIE Medical Imaging Conference 1999. SPIE 1999;3661:541–52.
26. Kawata Y, Niki N, Ohmatsu H, Kusumoto M, Kakinuma R, Mori K, et al. Computer aided differential diagnosis of pulmonary nodules based on a hybrid classification approach. In: Proceedings of SPIE Medical Imaging Conference 2001. SPIE 2001;4322:1796–806.
27. McNitt-Gray M, Hart E, Wyckoff N, Sayre J, Goldin J, Aberle A. A pattern classification approach to characterizing solitary pulmonary nodules imaged on high resolution CT: preliminary results. Med Phys 1999;26:880–8.
28. Fan L, Nowak C, Qian J, Kohl G, Naidich D. Automatic detection of lung nodules from multi-slice low-dose CT images. In: Proceedings of SPIE Medical Imaging Conference 2001. SPIE 2001;4322:1828–35.
29. Novak C, Fan L, Qian J, Kohl G, Naidich D. An interactive system for CT lung nodule identification and examination. In: Proceedings of International Conference on Computer Assisted Radiology and Surgery CARS 2001. Amsterdam, The Netherlands: Elsevier, 2001:599–604.
30. Wiemker R, Rogalla P, Zwartkruis A, Blaffert T. Computer aided lung nodule detection on high resolution CT data. In: Proceedings of SPIE Medical Imaging 2002. SPIE 2002;4684:677–88.
31. Novak CL, Qian J, Fan L, Naidich D, Ko JP, Rubinowitz AN. Inter-observer variations on interpretation of multislice CT lung-cancer screening studies and the implications for computer-aided diagnosis. In: Proceedings of SPIE Medical Imaging Conference 2002. SPIE 2002;4680:68–79.
32. Lawler LP, Wood SA, Pannu HS, Fishman EK. Computer-assisted detection of pulmonary nodules: preliminary observations using a prototype system with multidetector-row CT data sets. J Digit Imaging 2003;16:251–61.
33. Naidich DP, Ko JP, Stoeckel J, Abinanti N, Lu S, Moses D, et al. Computer-aided diagnosis: impact on nodule detection among community level radiologists. A multi-reader study. In: Proceedings of Computer Assisted Radiology and Surgery CARS 2004. Amsterdam, The Netherlands: Elsevier, 2004:902–7.
34. Clarke LP, Croft BY, Staab E. New NCI initiatives in computer aided diagnosis. In: Proceedings of SPIE Medical Imaging Conference 2000. SPIE 2000;3976:370–3.
35. Fischbach F, Knollmann F, Griesshaber V, Freund T, Akkol E, Felix R. Detection of pulmonary nodules by multislice computed tomography: improved detection rate with reduced slice thickness. Eur Radiol 2003;13:2378–83.
36. Zhao B, Yankelevitz D, Reeves A, Henschke C. Two-dimensional multi-criterion segmentation of pulmonary nodules on helical CT-images. Med Phys 1999;26:889–95.
37. Wormanns D, Kohl G, Klotz E, Heindel W, Diederich S. Clinical evaluation of the reproducibility of volume measurements of pulmonary nodules. In: Proceedings of SPIE Medical Imaging 2002. SPIE 2002;4684:316–22.
38. Fan L, Qian J, Odry B, Shen H, Naidich D, Kohl G, et al. Automatic segmentation of pulmonary nodules by using dynamic 3D cross-correlation for interactive CAD systems. In: Proceedings of SPIE Medical Imaging 2002. SPIE 2002;4684:1362–9.
39. Wiemker R, Rogalla P, Hein E, Blaffert T, Rösch P. Computer aided segmentation of pulmonary nodules: automated vasculature cutoff in thick- and thinslice CT. In: Proceedings of Computer Assisted Radiology and Surgery, CARS 2003. Amsterdam, The Netherlands: Elsevier, 2003:965–790.
40. Wiemker R, Zwartkruis A. Optimal thresholding for 3D segmentation of pulmonary nodules in high resolution CT. In: Proceedings of International Conference on Computer Assisted Radiology and Surgery CARS 2001. Amsterdam, The Netherlands: Elsevier Publishers, 2001:653–8.
41. Hay O, Sifri D, Srinivas Y, Wiemker R. Evaluation of automatic volumetric segmentation of lung nodules in standard and low dose CT scans. Annual Meeting of the Radiological Society of North America RSNA 2003.
42. Blaffert T, Wiemker R. Comparison of different follow-up lung registration methods with and without segmentation. In: Proceedings of SPIE Medical Imaging Conference 2004. SPIE 2004;5370:1701–8.

43. Shah E, Blaffert T, Subramanyan K, Durgan J, Pohlman S. Automatic matching of the pulmonary nodules in current and former CT studies: a clinical evaluation. In: Proceedings of Computer Assisted Radiology and Surgery CARS 2004. Amsterdam, The Netherlands: Elsevier, 2004:941–5.
44. Betke M, Hong H, Thomas D, Prince C, Ko JP. Landmark detection in the chest and registration of lung surfaces with an application to nodule registration. Med Image Anal 2003;7:265–81.
45. Shen H, Fan L, Qian J, Odry BL, Novak CL, Naidich DP. Real-time and automatic matching of pulmonary nodules in follow-up multi-slice CT studies. In: Proceedings of the International Conference on Diagnostic Imaging and Analysis; 2002 August 18–20; Shanghai, China. 2002:101–6.